A bifurcation giving birth to order in an impulsively driven complex system

Akshay Seshadri and R. I. Sujith

Citation: Chaos **26**, 083103 (2016); doi: 10.1063/1.4958925
View online: http://dx.doi.org/10.1063/1.4958925
View Table of Contents: http://aip.scitation.org/toc/cha/26/8
Published by the American Institute of Physics

A bifurcation giving birth to order in an impulsively driven complex system

Akshay Seshadri[a] and R. I. Sujith[b]
Indian Institute of Technology Madras, Chennai, India

(Received 5 March 2016; accepted 16 June 2016; published online 3 August 2016)

Nonlinear oscillations lie at the heart of numerous complex systems. Impulsive forcing arises naturally in many scenarios, and we endeavour to study nonlinear oscillators subject to such forcing. We model these kicked oscillatory systems as a piecewise smooth dynamical system, whereby their dynamics can be investigated. We investigate the problem of pattern formation in a turbulent combustion system and apply this formalism with the aim of explaining the observed dynamics. We identify that the transition of this system from low amplitude chaotic oscillations to large amplitude periodic oscillations is the result of a discontinuity induced bifurcation. Further, we provide an explanation for the occurrence of intermittent oscillations in the system. *Published by AIP Publishing*. [http://dx.doi.org/10.1063/1.4958925]

Impulsive forcing of oscillatory systems can occur naturally in various situations. Rich dynamics is observed in kicked oscillatory systems, and we consider a turbulent combustion system which can be modelled as a kicked oscillator. Such combustion systems are usually plagued by the problem of large amplitude, self-sustaining periodic oscillations, commonly known as thermoacoustic instability. These oscillations are detrimental to the operation and performance of combustion systems and sometimes have serious consequences such as failure of space missions and shutting down of gas turbines in power plants. Stable combustion corresponds to low amplitude aperiodic fluctuations, but a change in some parameter of the system can cause the system to transition to thermoacoustic instability. A recent discovery shows that intermittency, a dynamical state composed of small amplitude aperiodic fluctuations and large amplitude periodic oscillations, is seen to portend thermoacoustic instability. The aim is to study this transition; however, due to the discontinuities endowed on the dynamics by kicked oscillatory modelling of the system, we cannot readily inspect the model in the parlance of smooth dynamical systems theory. For this reason, we adopt a dynamical systems theory framework that is capable of handling discontinuities, to explain the dynamics seen in the considered system. We show that the transition of this system from chaos to periodic oscillations is because of a discontinuity induced bifurcation. We also provide an explanation for the occurrence of intermittent periodic oscillations in the system.

I. INTRODUCTION

Studying oscillatory phenomena is indispensable if one has to understand the behaviour of a large number of complex systems. Many physical,[1–3] chemical,[4,5] and biological systems[6,7] display oscillatory behaviour and these oscillations can be very complex. In many cases, a natural choice to model systems involves forcing the oscillators by impulses or kicks. Such kicked oscillators have been used in studying various phenomena in science, a few examples being kicked quantum rotors,[8] kicked Bose-Einstein condensates,[9] radiative kicking of a charged particle,[10] and combustion systems.[11] It is well known that such systems can display a wide variety of dynamical features ranging from chaos to intermittency and limit cycles.[12–15] The majority of these studies deal, however, with linear oscillators or integrable systems with periodic forcing. A common technique employed to study their dynamics is to reduce them to a map.

Most oscillatory systems found in nature, however, are nonlinear, and the times at which the oscillators are kicked can display variation. In such situations, it is generally not possible to reduce the oscillator to a map. With the intention of studying the dynamics of such oscillations, we propose a framework which deals with oscillatory systems that are forced impulsively and where the kicking times can vary. To this end, we resort to piecewise smooth (PWS) dynamical systems theory, which allows for possible discontinuities in the system dynamics. A PWS dynamical system is one where the domain of the flow in partitioned into a finite number of regions and the flow in each of these partitions is smooth.[16,17] However, the crossing over of the flow from one region to another can occur in a discontinuous fashion.[16,17] The vector field that governs the flow in each of these partitions is also usually different.[16,17] The surface separating any two partitions is termed a discontinuity boundary. di Bernardo *et al.*[16] provide an excellent review of the subject and can be referred for technical details.

II. KICKED OSCILLATORS

We consider an oscillator described by the equation $\dot{\boldsymbol{x}} = \boldsymbol{f}(\boldsymbol{x})$, $\boldsymbol{x} \in \mathbb{R}^n$ and subject this oscillator to impulsive forcing, resulting in the following equation:

$$\dot{\boldsymbol{x}} = \boldsymbol{f}(\boldsymbol{x}) + \sum_{i \in T \subset \mathbb{N}} \boldsymbol{y}\, |\dot{g}_i(\boldsymbol{x})| \delta(g_i(\boldsymbol{x})). \tag{1}$$

This equation represents the kicking of the oscillator by an amount $\boldsymbol{y}$ when the state vector $\boldsymbol{x}$ satisfies the condition

[a]Electronic mail: akshayseshadri@gmail.com
[b]Electronic mail: sujith@iitm.ac.in

$g_i(\boldsymbol{x}) = 0$. $\boldsymbol{y}$ can be a constant or can take a value that depends on the state vector. It is easy to see that most kicked oscillators can be cast in the above form. We give a few examples to make this concrete.

Take the case of a simple harmonic oscillator that is forced periodically with a period T

$$\ddot{x} + \zeta\omega\dot{x} + \omega^2 x = \sum_{n\in N\subset\mathbb{N}} \sin(kx)\delta(t - nT).$$

The state vector for such a system is $\boldsymbol{x} = (x, \dot{x}, t) \in \mathbb{R}^3$, and when the condition $\boldsymbol{x}.\boldsymbol{e_3} - nT = 0$, $n \in N$, is satisfied, the system is forced impulsively. Here, $\boldsymbol{e_i}$ is the standard unit vector in the direction of the ith component. The system, in this case, is kicked by an amount $(0, \sin(k\boldsymbol{x}.\boldsymbol{e_1}), 0)$. The same can be done for, say, a Van der Pol oscillator with kicking.

We now analyze Equation (1) in parlance of PWS dynamical systems theory. We let the surfaces $\Sigma_i = \{\boldsymbol{x} \in \mathbb{R}^n | \, g_i(\boldsymbol{x}) = 0\}$ be the discontinuity boundaries. When the state vector is on one such surface, the oscillator satisfies the condition for kicking. Corresponding to this, we introduce the reset map $\mathcal{K}(\boldsymbol{x}) = \boldsymbol{x} + \boldsymbol{y}$ to account for the kicking. In regions between any two discontinuity boundaries, the flow is simply given as $\dot{\boldsymbol{x}} = \boldsymbol{f}(\boldsymbol{x})$. PWS dynamical systems in which a reset map is introduced at the discontinuity boundary are termed PWS hybrid systems.[17] The impact oscillator[16] is a standard example of PWS hybrid system, which has been extensively studied. The impact oscillator is constrained to lie on one region of the phase space due to the presence of a rigid impacting surface. Let the impacting surface be at $x = 0$; the impact changes the velocity of the oscillator from $\dot{x}$ to $-e\dot{x}$, where e is the coefficient of restitution. Then the state vector is $\boldsymbol{x} = (x, \dot{x}) \in \mathbb{R}^2$ and the condition for forcing to occur is $g(\boldsymbol{x}) \equiv \boldsymbol{x}.e_1 = 0$ and correspondingly, $\boldsymbol{y} = (0, -(1 + e)\boldsymbol{x}.\boldsymbol{e_2})$.

Returning to the case of kicked simple harmonic oscillator, we see that the surface $g_n(\boldsymbol{x}) \equiv \boldsymbol{x}.\boldsymbol{e_3} - nT = 0$ is a discontinuity boundary, and when the state vector lies on the discontinuity boundary, we apply the reset map $R(\boldsymbol{x}) = \boldsymbol{x} + \sin(k\boldsymbol{x}.\boldsymbol{e_1})\boldsymbol{e_2}$. Between any two kicks, the system evolves as per

$$\dot{\boldsymbol{x}} = \begin{pmatrix} 0 & 1 & 0 \\ -\omega^2 & -\zeta\omega & 0 \\ 0 & 0 & 0 \end{pmatrix} \boldsymbol{x} + \begin{pmatrix} 0 \\ 0 \\ 1 \end{pmatrix}.$$

A similar approach can be adopted for describing the impact oscillator. More complicated nonlinear systems can be modelled in the above form; however, properly defining the discontinuity boundaries and the reset maps might be specific to the system and should be handled appropriately.

Armed with this formalism, we can now tackle a more complicated problem: pattern formation in a turbulent combustion system. We start with a reduced-order model[15] that describes this system and rewrite it as a PWS dynamical system. The system turns out to be similar to the system defined by Equation (1), but with a slightly more complex structure.

III. PATTERN FORMATION IN TURBULENT COMBUSTION SYSTEM

We consider a turbulent fluid undergoing combustion in a confined environment in the presence of vortex shedding. This system is known to go from a disordered state to an organized state with a change in some control parameter.[18,19] In general, the disordered state of a thermoacoustic system can be considered noisy;[20,21] however, for the particular system we consider,[19] it has been shown that the disordered state corresponds to chaotic oscillations.[18,22] The system under consideration transitions from a chaotic state, where the oscillations are of low amplitude, to a state displaying large amplitude limit cycle oscillations.[18] This transition is marked by the presence of intermittency, where low amplitude aperiodic fluctuations are found along with large amplitude periodic oscillations.[19]

In this system, there is a three-way coupling between the acoustic pressure oscillations in the duct, the unsteady heat release rate oscillations, and hydrodynamics. The interaction between them results in large amplitude limit cycle oscillations, known as thermoacoustic instability. There are spatio-temporal patterns in the system during thermoacoustic instability;[23] however, we restrict ourselves to studying the temporal patterns observed in the system. We investigate a reduced-order model[15] that describes this system.

A. Model

The model deals with the flow in a duct of length L, where vortices are shed from a step at the inlet end (Figure 1). These vortices carry unburnt fuel and convect with the flow. The fuel in the vortices burn when the latter reach a distance L_c from the inlet end, leading to an instantaneous heat release rate. The acoustic pressure (p') and velocity (u') oscillations in the duct are decomposed in terms of the natural modes of the duct[11,15]

$$\begin{aligned} p'(x,t) &= \bar{p}\sum_{n=1}^{N} \frac{\dot{\eta}_n(t)}{\omega_n} \cos(\omega_n x/c) \quad \text{and} \\ u'(x,t) &= \frac{\bar{p}}{\bar{\rho}c}\sum_{n=1}^{N} \eta_n(t) \sin(\omega_n x/c). \end{aligned} \tag{2}$$

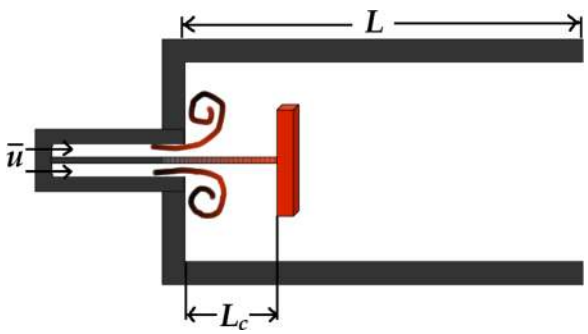

FIG. 1. A schematic of a combustor with a bluff-body at a distance L_c from the inlet. The combustor is a duct of length L, and vortices are shed from the inlet. Vortices burn when they impinge on the bluff-body. $\bar{u}$ is the mean velocity of the flow. All horizontal distances are measured from the inlet end.

Here, $\bar{p}$ is the mean pressure, $\bar{\rho}$ is the mean density, and c is the speed of sound. $\eta_n(t)$ and $\dot{\eta}_n(t)$ are the time-varying components of acoustic velocity and pressure and ω_n is the natural frequency of the nth acoustic mode.

Using the conservation equations, we obtain an oscillatory equation for these modes[11,15]

$$\ddot{\eta}_n + \xi_n \dot{\eta}_n + \omega_n^2 \eta_n = B_n \sum_j \delta(t - t_j), \quad n = \{1, 2, ..., N\}. \tag{3}$$

The kicking of these oscillators is due to the instantaneous burning of a vortex when it reaches the combustion location L_c. B_n is constant for a given mode and proportional to the mean velocity $\bar{u}$.[11,15] A vortex is shed at the inlet end depending on the value of the circulation Γ at the step. The circulation builds up at the step according to[15]

$$\frac{d\Gamma}{dt} = \frac{\bar{u}^2}{2} + \sum_j k_p \, p'(L_c, t_j) \, \delta(t - t_j - \tau), \tag{4}$$

and a vortex is shed if this circulation exceeds a critical value $\Gamma_{cr} = \Gamma_o \bar{u}$,[11,15] where Γ_o is a constant. The second term in Equation (4) describes the delayed feedback of acoustics on circulation build-up, due to the burning of vortices at time instants $\{t_j\}$.[15] k_p is an empirical constant that decides the strength of the acoustic feedback.[15] The jth shed vortex convects with the flow as described by the equation[15]

$$\frac{dx_j}{dt} = \alpha \bar{u} + u'(x_j, t), \tag{5}$$

where x_j is the location of the jth vortex and α is a constant that decides the mean convection speed of the vortices. These vortices move downstream, and when they reach L_c, they contribute to the kicking of the acoustic modes, thus forming a closed-loop of interaction. Refer Seshadri *et al.*[15] for a more detailed description. We assume here for simplicity that the time delay $\tau = L_c/c$ is negligible and this is true when $L_c/c \ll 1$ (which is the case in this study). We also make a note that k_p is in general a step function of the mean velocity;[15] however, because of the particular choice of k_p,[15] it is constant during the passage of the system from chaos to limit cycle oscillations and we treat it as such. The system transitions from low amplitude chaotic oscillations to large amplitude limit cycle oscillations with an increase in the mean velocity ($\bar{u}$), the control parameter, as seen in Figure 2. We also see intermittency in the system (Figure 2(b)), wherein low amplitude aperiodic fluctuations are sandwiched between large amplitude periodic bursts.

Equations (3)–(5) are solved using Runge-Kutta method of order 4 with a time-step of 10^{-5} s. The parameters used for solving the equations are the same as those utilized in Seshadri *et al.*,[15] except that the time delay τ is set to zero here. All the plots related to the model that we have used in this study have been obtained by solving the aforementioned set of equations.

B. The model as a PWS dynamical system

We express the model described above as a PWS dynamical system with the objective of investigating its dynamics. We form the vectors $\boldsymbol{\eta} = (\eta_1, \eta_2, ..., \eta_N)^T \in \mathbb{R}^N$ and $\dot{\boldsymbol{\eta}} = (\dot{\eta}_1, \dot{\eta}_2, ..., \dot{\eta}_N)^T \in \mathbb{R}^N$ from the acoustic modes and define $\boldsymbol{\Gamma}_v \in \mathbb{R}^M$ and $\boldsymbol{x}_v \in \mathbb{R}^M$ to be the vectors which, except for their first component, hold information about the circulation and position of all the vortices that will be shed. Strictly speaking, the vectors $\boldsymbol{\Gamma}_v$ and $\boldsymbol{x}_v$ must have countably infinite components; however, to avoid the mathematical intricacies associated with infinite dimensional vector spaces, we restrict to a large but finite dimension M. We then define the phase space of the complete system to be the direct sum of the spaces associated with the vectors $\boldsymbol{\Gamma}_v$, $\boldsymbol{x}_v$, $\boldsymbol{\eta}$, and $\dot{\boldsymbol{\eta}}$, i.e., the state vector of the system is $\boldsymbol{x} = (\boldsymbol{\Gamma}_v, \boldsymbol{x}_v, \boldsymbol{\eta}, \dot{\boldsymbol{\eta}}) \in \mathbb{R}^{2M+2N}$. We define the regions $\mathcal{R}_{sb}$ in the phase space, where flow exists, as

$$\begin{aligned} \mathcal{R}_{sb} = \{\boldsymbol{x} \in \mathbb{R}^{2M+2N} \,|\, & x_i > 0 \,\forall i = 1, 2, .., s \quad \text{and } x_{M+j} > L_c \,\forall j = 1, 2, ..., b; \\ & x_i < 0 \,\forall i = s+1, .., M \quad \text{and } x_{M+j} < L_c \,\forall j = b+1, ..., M; \\ & 1 \le b \le s \le M - 1\}, \end{aligned} \tag{6}$$

where x_i is the ith component of $\boldsymbol{x}$. That is, in the region $\mathcal{R}_{sb}$, the first s components of $\boldsymbol{\Gamma}_v$ are positive and the first b components of $\boldsymbol{x}_v$ are greater than L_c. The presence of the state vector in the region $\mathcal{R}_{sb}$ signifies that $s-1$ vortices have shed and $b-1$ vortices have burnt. We require any initial condition of the system to be of the form $\boldsymbol{x}_o = (\boldsymbol{\Gamma}_{v_o}, \boldsymbol{x}_{v_o}, \boldsymbol{\eta}_o, \dot{\boldsymbol{\eta}}_o)$, where $\boldsymbol{\Gamma}_{v_o} = (\epsilon, -\Gamma_{cr}, -\Gamma_{cr}, ..., -\Gamma_{cr})^T$ and $\boldsymbol{x}_{v_o} = (L_c + \epsilon, 0, 0, ..., 0)^T, \epsilon > 0$. Such a choice for initial values of $\boldsymbol{\Gamma}_{v_o}$ and $\boldsymbol{x}_{v_o}$ resembles the situation where the circulation build-up at the step has not started. Note that we have translated the value of Γ by Γ_{cr}; this is possible since such a translation does not affect the overall dynamics (see Equation (4)). We chose $\epsilon > 0$ and $L_c + \epsilon > 0$ as the first component of $\boldsymbol{\Gamma}_{v_o}$ and $\boldsymbol{x}_{v_o}$ so that $\boldsymbol{x}_o \in \mathcal{R}_{11}$.

With the above definitions in place, the continuous part of the equations of the model can be expressed in a compact form as

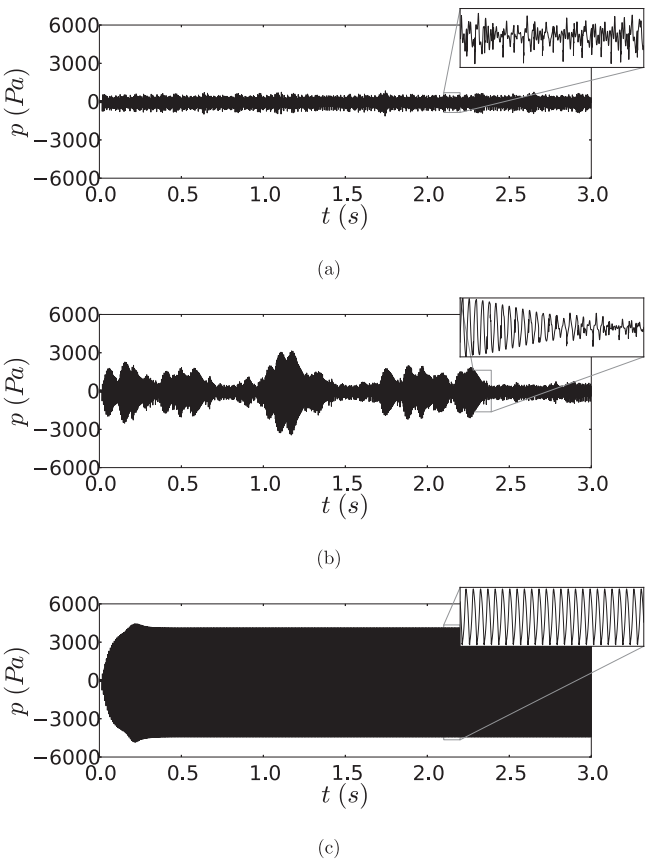

FIG. 2. Plot of acoustic pressure varying with time for (a) $\bar{u} = 10.0\,\mathrm{m/s}$ showing chaos, (b) $\bar{u} = 10.5\,\mathrm{m/s}$ showing intermittency, and (c) $\bar{u} = 10.7\,\mathrm{m/s}$ showing limit cycle oscillations. The system undergoes a bifurcation from chaos to limit cycle via intermittent oscillations. Refer Seshadri *et al.*[15] for the list of parameter values used. The time delay (τ) has been set to zero. An initial condition of $\eta_1 = 0.001$, with the rest of the acoustic modes set to zero, has been used.

$$\dot{\boldsymbol{x}} = \begin{cases} A\boldsymbol{x} + \dfrac{\bar{u}^2}{2}\boldsymbol{s} + \alpha\bar{u}\boldsymbol{b} + U\boldsymbol{x} & \text{if } \boldsymbol{x} \in \mathcal{R}_{sb} \\ 0 & \text{if } \boldsymbol{x} \notin \bigcup_{s,b=1}^{M-1} \mathcal{R}_{sb}, \end{cases} \tag{7}$$

$$A = \begin{pmatrix} 0_{M\times M} & 0_{M\times M} & 0_{M\times N} & 0_{M\times N} \\ 0_{M\times M} & 0_{M\times M} & 0_{M\times N} & 0_{M\times N} \\ 0_{N\times M} & 0_{N\times M} & 0_{N\times N} & \mathbb{I}_{N\times N} \\ 0_{N\times M} & 0_{N\times M} & -\boldsymbol{\omega}_{N\times N} & -\boldsymbol{\xi}_{N\times N} \end{pmatrix},$$

$$U = \begin{pmatrix} 0_{M\times M} & 0_{M\times M} & 0_{M\times N} & 0_{M\times N} \\ 0_{M\times M} & 0_{M\times M} & \boldsymbol{S}_{M\times N} & 0_{M\times N} \\ 0_{N\times M} & 0_{N\times M} & 0_{N\times N} & 0_{N\times N} \\ 0_{N\times M} & 0_{N\times M} & 0_{N\times N} & 0_{N\times N} \end{pmatrix}. \tag{8}$$

Here, 0 is a matrix with all elements zero, $\mathbb{I}$ is the identity matrix, and $\boldsymbol{\omega} = \mathrm{diag}(\omega_1^2, \omega_2^2, ..., \omega_N^2)$, $\boldsymbol{\xi} = \mathrm{diag}(\xi_1, \xi_2, ..., \xi_N)$ are diagonal matrices. $s_{ij} = (\bar{p}/\bar{\rho}c)\sin(\omega_j x_{M+i}/c)$ for $s+1 \le i \le b$, while $s_{ij} = 0$ for other i are the elements of $\boldsymbol{S}$, which is the matrix that accounts for the acoustic velocity (u'). Further, $\boldsymbol{s}$ is a vector with the $(s+1)$th component 1 and the rest 0 and $\boldsymbol{b}$ is a vector with the components from $M+b+1$ up to and including $M+s$ equal to 1 and the rest zero. Therefore, discontinuity in the flow comes when some component of $\boldsymbol{\Gamma_v}$ or $\boldsymbol{x_v}$ becomes positive or exceeds L_c, respectively. Associated with this event, we define the two discontinuity boundaries

$$\Sigma_s = \left\{\boldsymbol{x} \in \mathbb{R}^{2M+2N} \,|\, x_s = 0\right\}; \quad s \in \{1, ..., M\}, \tag{9}$$

$$\bar{\Sigma}_b = \left\{\boldsymbol{x} \in \mathbb{R}^{2M+2N} \,|\, x_{M+b} = L_c\right\}; \quad b \in \{1, ..., M\}. \tag{10}$$

One would have noticed by this point that the equations of the model are more complex than that defined by Equation (1). This is because the vector field itself changes as we move from one region to another, apart from the discontinuity arising due to kicking. On the surfaces Σ_s and $\bar{\Sigma}_b$, we can define the vector field to be the same as that in the region $\mathcal{R}_{sb}$. Owing to our definition of the evolution of the flow (Equation (7)), there will be no motion along the discontinuity boundaries.

When the state vector reaches Σ_s, it signifies the shedding of $(s-1)$th vortex. On the other hand, the state vector crossing $\bar{\Sigma}_b$, from $\mathcal{R}_{sb-1}$ to $\mathcal{R}_{sb}$, indicates the burning of the $(b-1)$th vortex, i.e., the impingement of the vortex on the bluff-body at a distance L_c from the inlet. Corresponding to this impingement of the vortex, we need to add a kick to the pressure oscillations as well as to the circulation building up at the step (see Equations (3) and (4)). Hence we introduce a reset map $\mathcal{K} : \bar{\Sigma}_b \to \bar{\Sigma}_b$ to account for these kicks

$$\mathcal{K}(\boldsymbol{x}) = \boldsymbol{x} + P_c\boldsymbol{s} + \boldsymbol{H_p}, \quad \boldsymbol{x} \in \bar{\Sigma}_b, \tag{11}$$

$$P_c = \bar{p}\,k_p \sum_{j=1}^{N} \left(\dot{\eta}_j + B_j\right) \frac{\cos\left(\omega_j L_c/c\right)}{\omega_j}. \tag{12}$$

As before, $\boldsymbol{s}$ is the vector with $(s+1)$th component 1 and the rest zero. $\boldsymbol{H_p}$ is a constant vector with B_n along the $\dot{\boldsymbol{\eta}}$ coordinate directions, the rest of the components being zero, i.e., $\boldsymbol{H_p} = (0, ..., 0, B_1, B_2, ..., B_N)^T$. $\boldsymbol{H_P}$ shows the effect of heat release rate on the pressure oscillations upon the impingement of a vortex, while $P_c\boldsymbol{s}$ shows the feedback of the pressure on circulation building up at the step.

Having re-framed the original set of equations as a PWS dynamical system, a few remarks are in order. We note that the proposed PWS dynamical system representation is only an approximate one. This is because we define the vectors $\boldsymbol{\Gamma_v}$ and $\boldsymbol{x_v}$ to hold information about all the vortices that will ever be formed. Clearly then, these vectors must have countably infinite components. However, we have restricted these vectors to a finite (M) number of components, which makes the description approximate. However, since the dimension M can be chosen to be very large, we can satisfactorily describe the dynamics for a finite time evolution of the system. For obtaining the solutions numerically, the maximum value of M that one needs to choose is equal to the total number of time steps, since in the extreme scenario, one vortex will be shed at every time instant. On the other hand, if we have the constraint that only a finite number of vortices are going to be shed, then M is surely finite. In any case, as long

as the actual flow does not change its structure qualitatively in the asymptotic limit, which is the expected behaviour, we can resort to the current description.

IV. BIFURCATION

We can now investigate the transition to order that occurs in the system. Note that we only provide a qualitative description of the bifurcation and make no attempt to derive the normal form. We restrict our study to the subspace spanned by the vectors $\boldsymbol{\eta}$ and $\dot{\boldsymbol{\eta}}$, since the dynamics of interest occurs only in this region. All the parameters of the model are chosen such that we observe a transition from low amplitude chaotic oscillations, to intermittency and then finally large amplitude limit cycle oscillations; we do not focus on any other form of transition here, even if it is displayed by the system. We make a note that the contribution of the acoustic velocity u' is negligible, at least for low mean velocities, in affecting the motion of shed vortices (Equation (5)). This is because all the vortices are confined to a region close to the inlet end (as long as $L_c/L \ll 1$, which is true in this study), resulting in a small value of the sine component which appears in u' (see Equation (2)). In this regard, we discard, for most part of the discussion that follows, the contribution of u' in explaining the dynamics of the system.

As mentioned earlier, the system starts off in a chaotic state, where the pressure oscillations are of small amplitude (Figure 2(a)). In this case, the burning times of the vortices, $\{t_j\}$, vary significantly and these are usually not close to the time period of the acoustic oscillator $(\eta_n, \dot{\eta}_n)$.[15] As a result, the pressure oscillations behave in an aperiodic fashion (see Equation (3)) and consequently affect the circulation in an irregular manner (see Equation (4)). Since the value of circulation dictates vortex shedding, the times of vortex shedding are sporadic which is reflected in $\{t_j\}$. This mutual interaction between the aperiodic pressure oscillations and the times of vortex burning is the reason for the chaotic oscillations observed in the system.

With increasing mean velocity $\bar{u}$, intermittent oscillations are seen in the system (Figure 2(b)). Here, the pressure oscillations display low amplitude aperiodic fluctuations interspersed with bursts of large amplitude periodic oscillations. This is due to two main reasons: the increase in $\bar{u}$ changes Equation (7) such that $T_{v,n} = nL_c/\alpha\bar{u}$, for some $n \in \mathbb{Q}$, is closer to the acoustic time period $T_a = 2\pi/\omega_1$ and it also increases the value of the components of $\boldsymbol{H_p}$ (note that $B_n \propto \bar{u}$). We incorporate n in $T_{v,n}$ to address the possibility of modes other than the fundamental modes coming close to each other. When we say, $T_{v,n}$ and T_a are close, we mean $\epsilon_{i1} \leq |T_{v,n} - T_a| \leq \epsilon_{i2}$, where ϵ_{i1} and ϵ_{i2} are much smaller than both $T_{v,n}$ and T_a. However, the specific values of ϵ_{i1}, ϵ_{i2} depend on the parameters we choose. Now, because the frequency of impingement of vortices is close to the acoustic frequency, the acoustic oscillator is excited at a frequency close to its natural frequency. Consequently, the resultant pressure oscillations are large in amplitude. The increase in the value of $\boldsymbol{H_p}$ is such that when the state vector $\boldsymbol{x}$ is on the discontinuity boundary $\bar{\Sigma}_b$, the magnitude of pressure oscillations ($\dot{\boldsymbol{\eta}}$) is large enough for the reset map $\mathcal{K}$ to take $\boldsymbol{x}$ from $\mathcal{R}_{sb}$ to $\mathcal{R}_{(s+1)b}$. This physically corresponds to an instantaneous shedding of a vortex at the step. This shed vortex again impinges the bluff-body in a time $T_{v,n}$ (this is also the time for $\boldsymbol{x}$ to go from $\bar{\Sigma}_b$ to $\bar{\Sigma}_{b+1}$). However, if the difference in $T_{v,n}$ and T_a is not small enough (due to the restriction placed by ϵ_{i1}), vortex impingements and acoustic oscillations will eventually go out of phase; at a certain point, the magnitude of pressure oscillations will not be enough for $\mathcal{K}$ to take $\boldsymbol{x}$ from $\mathcal{R}_{sb}$ to $\mathcal{R}_{(s+1)b}$. At this point, the system will start displaying aperiodic oscillations. The zoomed part of Figure 2(b) shows this gradual slipping of phase between vortex impingements and pressure oscillations, leading to aperiodic fluctuations. If at some later time, the impingement time is close to T_a and the magnitude of pressure oscillations is appropriate, large amplitude oscillations start again.

The presence of such dynamics during intermittency can be easily verified. To this end, we define a quantity S as follows. If the value of the acoustic feedback, resulting from the impingement of a vortex at L_c, can cause a vortex to shed instantaneously at the step, we assign a value of 1 to S. If the feedback is unable to shed a vortex instantaneously, we assign S the value 0. So a value of $S = 1$ implies that the reset map $\mathcal{K}$ takes the state vector $\boldsymbol{x} \in \bar{\Sigma}_b$ from the region $\mathcal{R}_{sb}$ to $\mathcal{R}_{(s+1)b}$. The plot of S as a function of time can be seen in Figure 3. We can see from Figure 3(a) that during the low amplitude aperiodic oscillations, the feedback almost never sheds a vortex instantaneously. Turning our attention to the large amplitude periodic burst in Figure 3(a), we can see that during the growth phase of burst, the value of S is 1. This

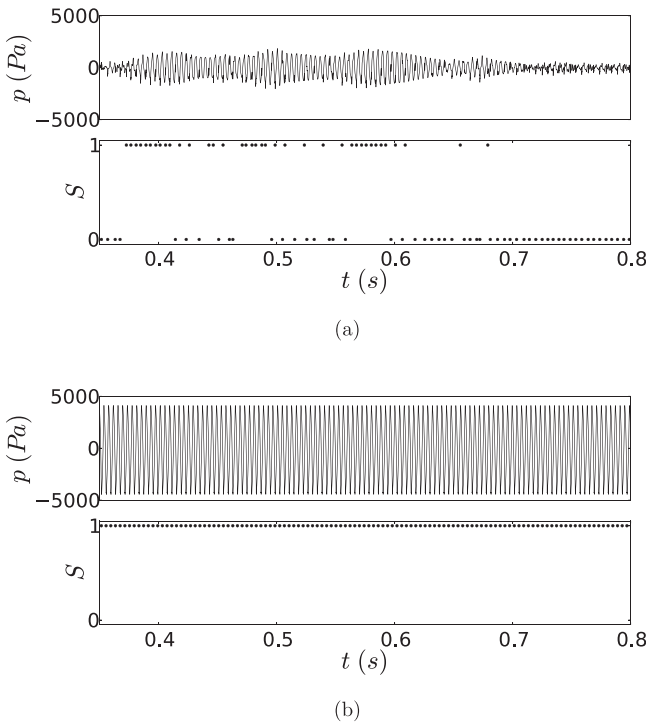

FIG. 3. Plot of S with time for (a) an intermittent signal at $\bar{u} = 10.5\,\mathrm{m/s}$ and for (b) limit cycle oscillations at $\bar{u} = 10.7\,\mathrm{m/s}$. A value of $S = 1$ implies the acoustic feedback on circulation leads to instantaneous shedding of a vortex at step, while a value of $S = 0$ shows that the feedback is unable to shed a vortex instantaneously. We can see that during sustained periodic oscillations, the feedback is strong enough to instantaneously shed a vortex.

continues till the pressure oscillations and the kicking go out of phase. Then, as described above, the magnitude of feedback is not enough to shed a vortex instantaneously. Thus we have a value of $S=0$ in the decay phase of the burst, as can be seen from Figure 3(a).

Finally, when the mean velocity is such that $T_{v,n}$ is very close or equal to T_a, limit cycle oscillations are observed (see Figure 2(c)). By this, we mean $|T_{v,n}-T_a| \leq \epsilon_l$, where $\epsilon_l \leq \epsilon_{i1}$. This is where the bifurcation occurs—the state vector $\boldsymbol{x}$ moves from $\bar{\Sigma}_b$ to $\bar{\Sigma}_{b+1}$ in a time close to $T_{v,n} \cong T_a$ and when $\boldsymbol{x}$ is on $\bar{\Sigma}_b$, the reset map $\mathcal{K}$ always takes it from $\mathcal{R}_{sb}$ to $\mathcal{R}_{(s+1)b}$. Since the arrival of $\boldsymbol{x}$ at $\bar{\Sigma}_b$ results in kicking of the acoustic oscillator, the oscillator is forced nearly at its natural frequency and consequently large amplitude oscillations are observed. In the preceding discussion, we have considered the case when a single vortex is present at a given time between the step and point of combustion. A similar argument can likely be presented when more than one vortex is present, but we do not enter into that discussion here. We also mention here that the acoustic velocity u' is not negligible during limit cycle oscillations; nevertheless, the above description holds true even in this case.

Again, we can verify from Figure 3(b) that during large amplitude limit cycle oscillations, $\boldsymbol{x} \in \bar{\Sigma}_b \cap \bar{\mathcal{R}}_{sb}$ implies $\mathcal{K}(\boldsymbol{x}) \in \bar{\Sigma}_b \cap \bar{\mathcal{R}}_{(s+1)b}$, that is, the acoustic feedback always succeeds in shedding a vortex instantaneously. This corresponds to the quantity S always having a value 1, which is evident from the figure. Further, to ascertain that when $T_{v,n}$ is close to T_a, we have intermittency and that, when they are nearly equal, we have limit cycle oscillations, we plot the bifurcation diagram in Figure 4. The peaks of the pressure signal have been plotted against the mean convection frequency (which we define as the inverse of $T_v = T_{v,1}$) in this figure. A black circle corresponds to the peak having an amplitude greater than some threshold (800 Pa in this case), while a hollow circle implies the peak has a value less than the defined threshold. We choose the amplitude threshold such that if, at some T_v, almost all circles are hollow, it means that the system exhibits low amplitude chaotic oscillations. If both hollow and black circles are present, we have intermittency and only a few black circles mean limit cycle oscillations. Such a choice of threshold is possible due to the nature of the transition in this system. We plot only a few peaks in the figure for better clarity.

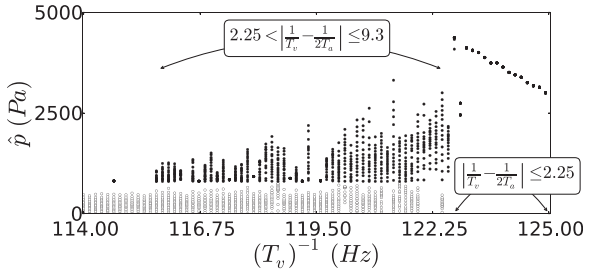

FIG. 4. Plot of peaks of pressure ($\hat{p}$) against the mean vortex convection frequency ($T_v^{-1} = \alpha\bar{u}/L_c$). Pressure time series of 1.4s duration has been considered, from which a transient of 0.05s has been subtracted. The acoustic frequency is 250 Hz or equivalently, $T_a = 0.004$s. The set of peaks has been undersampled to avoid cluttering the plot. Chaos, intermittency, and limit cycle oscillations correspond to different segments in the plot.

We see from Figure 4 that as $T_{v,1/2}$ approaches T_a, we have intermittency and limit cycle oscillations. This demonstrates that the mean vortex convection time (T_v) is almost twice the acoustic time period during limit cycle oscillations. However, for our choice of model parameters, we observe that there are two vortices present at a given time in between the step and L_c. These vortices are equally spaced, and due to this, the time difference between two consecutive impingement of vortices is nearly equal to T_a. Hence, our explanation of the bifurcation holds true here; the reason being, we can imagine the scenario to be that of one vortex present at a given time between step and L_c, but with $T_{v,1}$ (instead of $T_{v,1/2}$) close to T_a. We also see that the amplitude of limit cycle oscillations gradually decreases (Figure 4) and that maximum limit cycle oscillation amplitude is at $(T_v)^{-1} \approx 123$ Hz (call this T_m). It may come as a surprise that we have the maximum amplitude at T_m and not at $T_v = T_a$. This is, in effect, an artefact of u' not being negligible during limit cycle oscillations. It turns out that the time between two vortex impingements is equal to T_a at $T_v = T_m$, which explains why the amplitude is maximum here. This conveys that the time between two consecutive vortex impingements is a more faithful way of judging the system compared to $T_{v,n}$. However, the time between two impingements varies with time, and for this reason, we stick to a description that utilizes $T_{v,n}$. It is necessary to recognize that the bifurcation diagram we have plotted is not unique. The length and the portion of the time series as well as the initial conditions we use will affect its appearance. Nevertheless, it serves the purpose of illustrating the remarks we mentioned above.

A nice analogy can be drawn between the bifurcation we observe in this system and the saddle node bifurcation seen in a logistic map. Recall that the third iterate of the logistic map undergoes a saddle-node bifurcation (also called tangent bifurcation) prior to the onset of period-3 oscillations.[24] The map, just before periodic oscillations, shows intermittent behaviour when there is a bottleneck region present in the system (see Figure 5). When the trajectory enters this bottleneck region (the zoomed part in Figure 5(a)), near-periodic oscillations are seen but when it leaves this region, chaotic oscillations are observed again. This can be seen from Figure 5, where the return map of the third iterate of the logistic map and the corresponding trajectory is shown. When the bifurcation occurs, period-3 orbits are formed as the fixed points correspond to the third iterate of the map. We compare this scenario with the bifurcation seen in our system.

We can write the equations of our system, neglecting u', as follows:

$$\begin{aligned} \dot{\boldsymbol{x}} &= \left(A\boldsymbol{x} + \frac{\bar{u}^2}{2}\boldsymbol{s}\right) + \alpha\bar{u}\boldsymbol{b} && \text{if } \boldsymbol{x} \in \mathcal{R}_{sb}, \\ \mathcal{K}(\boldsymbol{x}) &= \boldsymbol{x} + P_c\boldsymbol{s} + \boldsymbol{H_p} && \text{if } \boldsymbol{x} \in \bar{\Sigma}_b, \\ \dot{\boldsymbol{x}} &= 0 && \text{otherwise.} \end{aligned}$$

Here, we have grouped the first two terms of $\dot{\boldsymbol{x}}$ and left out the term $\boldsymbol{r}_{\bar{u}} = \alpha\bar{u}\boldsymbol{b}$ so as to compare it with the normal form of the saddle node bifurcation, $\dot{x} = x^2 + r$. In our case, $\bar{u}$ is the bifurcation parameter, while r is the bifurcation

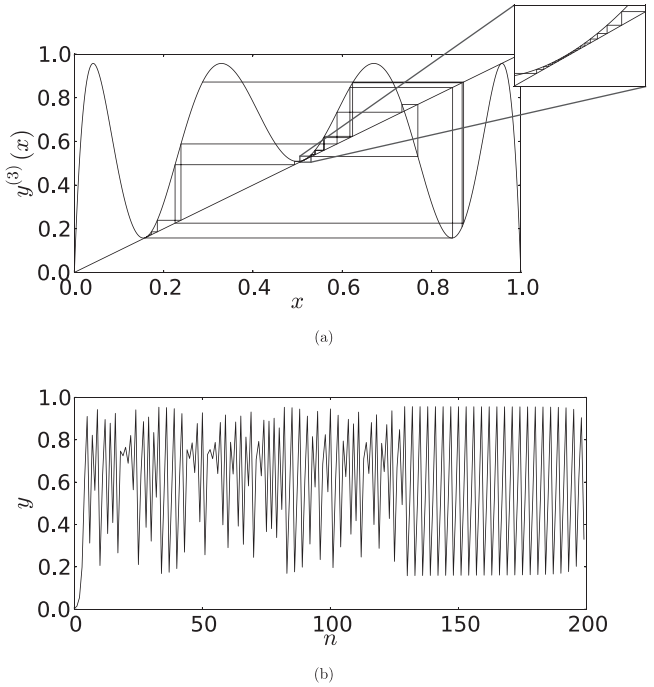

FIG. 5. Plot of (a) the third iterate ($y^{(3)}$) of the logistic map $y = rx(1-x)$ for $r = 3.8282$ and the orbit for an initial condition of $x_o = 0.001$ and (b) the corresponding trajectory of the logistic map displaying intermittency for the same r and initial condition. The zoomed inset in (a) shows the bottleneck region which forms just before the tangent bifurcation. Only a part of the trajectory is plotted in (a) for clarity.

parameter for saddle node bifurcation. Note that although $(\bar{u}^2/2)\boldsymbol{s}$ depends on $\bar{u}$, during limit cycle oscillations, it does not contribute to the dynamics since a vortex is shed as soon as $\boldsymbol{x}$ reaches $\bar{\Sigma}_b$. As $\bar{u}$ increases in our system, $\boldsymbol{r}_{\bar{u}}$ and $\boldsymbol{H_p}$ are directly affected. Increase in the magnitude of $\boldsymbol{r}_{\bar{u}}$ results in $T_{v,n}$ approaching T_a. $T_{v,n}$, and T_a becoming close enough can be thought of as entering a bottleneck region, where we observe intermittent oscillations. The closer $T_{v,n}$ is to T_a, the longer is the duration of the intermittent periodic bursts and so is the growth in their amplitude. This corresponds to the system spending more time in the bottleneck region. Hence, increase in $\bar{u}$, which results in the growth of magnitude of $\boldsymbol{r}_{\bar{u}}$, is responsible for a longer duration of the intermittent bursts. This is indeed observed in the model[15] and the experiments.[25] Finally when $T_{v,n}$ and T_a are almost equal, we observe limit cycle oscillations in the system.

We now take the liberty of listing a shortcoming of the formulation. Take a note that though we have chaotic and limit cycle oscillations in the $\boldsymbol{\eta}$ and $\dot{\boldsymbol{\eta}}$ subspaces, the same is not true for the original phase space. This is because these do not correspond to closed trajectories in the original phase space - the flow just moves from one region to the next and does not return to a previous region again. Despite this, we have a qualitative change in how the flow behaves in the original phase space during the bifurcation. Prior to the bifurcation, the flow moves haphazardly from one region to another; however, after the bifurcation, it takes equal amounts of time to move from one region to the next. Also note that this system may be capable of showing dynamics other than what has been discussed in this study. We, however, refrain from exploring this prospect.

We wish to point out that previous studies relating to this particular system have all been in the purview of smooth dynamical systems theory. However, the bifurcation responsible for the transition to combustion instability is essentially a discontinuity induced bifurcation, at least in the considered system. This prompts us to adopt the framework of PWS dynamical systems theory or some alternate framework that can handle discontinuities, for future studies pertaining to this system. Furthermore, though we have not derived the normal form for the bifurcation, we believe that this could be a previously uninvestigated bifurcation. This could also mean that the intermittency observed in this system is not one of the standard intermittencies that have been studied. Nonetheless, this is mere speculation at this juncture.

As an end note, we summarize the above analysis of the transition in an approximate, but simple, way.

(i) We have two main players: $\boldsymbol{r}_{\bar{u}}$ and $\mathcal{K}(\boldsymbol{x})$. $\boldsymbol{r}_{\bar{u}}$, the continuous part of the system, relates to the vortex convection time scale $T_{v,n}$, while $\mathcal{K}(\boldsymbol{x})$, the discontinuous part of the system, decides if the state vector is taken from the region $\mathcal{R}_{sb}$ to $\mathcal{R}_{(s+1)b}$. Changing $\bar{u}$ is equivalent to changing the magnitude of $\boldsymbol{r}_{\bar{u}}$, and this directly affects $T_{v,n}$.

(ii) When $\bar{u}$ increases such that the $T_{v,n}$ is close to the acoustic time period T_a, we have intermittent oscillations in the system. This is because, under appropriate conditions, $\mathcal{K}(\boldsymbol{x})$ acts after every $T_{v,n}$ interval of time, and takes $\boldsymbol{x}$ from the region $\mathcal{R}_{sb}$ to $\mathcal{R}_{(s+1)b}$. But since $T_{v,n}$ is not equal to T_a, the kicking and oscillations gradually slip out of phase and the periodic burst comes to an end, paving way for aperiodic oscillations. When the conditions are right again, the burst of periodic oscillations begins. Clearly, as $T_{v,n}$ and T_a come closer, the duration of the periodic bursts increases.

(iii) As $\bar{u}$ increases further and $T_{v,n}$ is almost equal to T_a, we have limit cycle oscillations in the system. Here, the reset map $\mathcal{K}(\boldsymbol{x})$ always takes $\boldsymbol{x}$ from the region $\mathcal{R}_{sb}$ to $\mathcal{R}_{(s+1)b}$ after a time period $T_{v,n}$ which is nearly equal to T_a. The result is periodic oscillations, and since the kicking frequency almost matches the acoustic frequency, the oscillations are large in amplitude.

This shows how the interplay between the continuous and discontinuous parts of the system results in the transition to limit cycle oscillations through the formation of intermittent periodic bursts.

ACKNOWLEDGMENTS

We thank ONRG for the financial support (Grant No. N62909-14-1-N299) provided for conducting this study.

[1]J. M. Dawson, Phys. Rev. **113**, 383 (1959).
[2]M. Golubitsky and W. Langford, Physica D: Nonlinear Phenom. **32**, 362 (1988).
[3]M. Van Exter and A. Lagendijk, Phys. Lett. A **99**, 1 (1983).
[4]M. Dolnik, I. Schreiber, and M. Marek, Phys. Lett. A **100**, 316 (1984).
[5]V. Petrov, Q. Ouyang, and H. L. Swinney, Nature **388**, 655 (1997).

[6]M. R. Guevara and L. Glass, J. Math. Biol. **14**, 1 (1982).
[7]R. FitzHugh, Biophys. J. **1**, 445 (1961).
[8]F. Moore, J. Robinson, C. Bharucha, B. Sundaram, and M. Raizen, Phys. Rev. Lett. **75**, 4598 (1995).
[9]C. Zhang, J. Liu, M. G. Raizen, and Q. Niu, Phys. Rev. Lett. **92**, 054101 (2004).
[10]Y. Ashkenazy and L. P. Horwitz, Fractals **10**, 353 (2002).
[11]K. I. Matveev and F. E. C. Culick, Combust. Sci. Technol. **175**, 1059 (2003).
[12]K. K. Lin and L.-S. Young, J. Fixed Point Theory Appl. **7**, 291 (2010).
[13]G. Zaslavsky, Phys. Lett. A **69**, 145 (1978).
[14]S. Abdullaev, Chaos **4**, 569 (1994).
[15]A. Seshadri, V. Nair, and R. Sujith, Combust. Theory Modell. **20**, 441 (2016).
[16]M. Di Bernardo, C. J. Budd, A. R. Champneys, P. Kowalczyk, A. B. Nordmark, G. O. Tost, and P. T. Piiroinen, SIAM Rev. **50**, 629 (2008).
[17]M. Bernardo, C. Budd, A. R. Champneys, and P. Kowalczyk, *Piecewise-Smooth Dynamical Systems: Theory and Applications* (Springer Science & Business Media, 2008), Vol. 163.
[18]V. Nair, G. Thampi, S. Karuppusamy, S. Gopalan, and R. Sujith, Int. J. Spray Combust. Dyn. **5**, 273 (2013).
[19]V. Nair, G. Thampi, and R. Sujith, J. Fluid Mech. **756**, 470 (2014).
[20]N. Noiray and B. Schuermans, Int. J. Non-Linear Mech. **50**, 152 (2013).
[21]N. Noiray and B. Schuermans, Proc. R. Soc. A **469**, 20120535 (2013).
[22]J. Tony, E. Gopalakrishnan, E. Sreelekha, and R. Sujith, Phys. Rev. E **92**, 062902 (2015).
[23]P.-H. Renard, D. Thevenin, J.-C. Rolon, and S. Candel, Prog. Energy Combust. Sci. **26**, 225 (2000).
[24]E. Ott, *Chaos in Dynamical Systems* (Cambridge University Press, 2002).
[25]V. Nair, G. Thampi, and R. Sujith, n3l International Summer School and Workshop on Non-Normal and Nonlinear Effects in Aero and Thermoacoustics (2013).